Cooperation and Competition in Synchronous Open Quantum Systems

Taufiq Murtadho,[1,2,3] Sai Vinjanampathy,[4,5,6,*] and Juzar Thingna[1,2,7,†]

[1]Center for Theoretical Physics of Complex Systems, Institute for Basic Science (IBS), Daejeon 34126, Republic of Korea
[2]Basic Science Program, Korea University of Science and Technology, Daejeon 34113, Republic of Korea
[3]School of Physical and Mathematical Sciences, Nanyang Technological University, 637371, Singapore
[4]Department of Physics, Indian Institute of Technology-Bombay, Powai, Mumbai 400076, India
[5]Centre of Excellence in Quantum Information, Computation, Science and Technology, Indian Institute of Technology Bombay, Powai, Mumbai 400076, India
[6]Centre for Quantum Technologies, National University of Singapore, 3 Science Drive 2, Singapore, Singapore
[7]Department of Physics and Applied Physics, University of Massachusetts, Lowell, Massachusetts 01854, USA

(Received 13 January 2023; accepted 13 June 2023; published 17 July 2023)

Synchronization between limit cycle oscillators can arise through entrainment to an external drive or through mutual coupling. The interplay between the two mechanisms has been studied in classical synchronizing systems, but not in quantum systems. Here, we point out that competition and cooperation between the two mechanisms can occur due to phase pulling and phase repulsion in quantum systems. We study their interplay in collectively driven degenerate quantum thermal machines and show that these mechanisms either cooperate or compete depending on the working mode of the machine (refrigerator or engine). The entrainment-mutual synchronization interplay persists with an increase in the number of degenerate levels, while in the thermodynamic limit of degeneracy, mutual synchronization dominates. Overall, our work investigates the effect of degeneracy and multilevel scaling of quantum synchronization and shows how different synchronizing mechanisms can cooperate and compete in quantum systems.

DOI: 10.1103/PhysRevLett.131.030401

Introduction.—Synchronization is a ubiquitous phenomenon in which stable phase relations emerge between multiple limit cycle oscillators [1]. There are two main mechanisms that give rise to synchronization: (i) *entrainment* that refers to the synchronization of an oscillator by unidirectional coupling to a periodic external drive [2] and (ii) *mutual synchronization* which refers to the adjustment of rhythms of two or more mutually coupled oscillators, such as in the widely known Kuramoto model [3]. These two mechanisms may coexist in some systems [4–7], and their interplay has also been experimentally studied in globally coupled electrochemical oscillators [8].

In the same spirit as classical synchronization, quantum synchronization is often studied through entrainment [9–14] or mutual coupling [15–21] and has been experimentally observed recently [22–24]. However, unlike classical synchronization, the coexistence and the interplay between these two mechanisms in the quantum regime have not been investigated. Understanding this interplay is crucial in the control of various quantum technologies where both driving and interaction are important such as in superradiant lasers [16], coupled time crystals [25], and coupled machines [26–33].

In this Letter, we show that the phases of steady-state coherence follow a phase synchronization model, where the external entraining drive competes with the mutually coupled phases. This opens up the possibility of observing well-studied classical phenomena, such as synchronization-antisynchronization transition [34] and chimeras [35,36], in the quantum regime. Our framework applies to generic quantum systems, with external drives that couple the coherences (coherently) that themselves are mutually coupled (dissipatively), leading to an interplay between entrainment and mutual synchronization.

As a concrete example, we consider a degenerate multilevel generalization of the Scovil–Schulz-DuBois maser heat engine [37,38], where the external collective drive connects transitions between the degenerate manifold and the first-excited state [38]. The states within the degenerate manifold form a *stable* collective symmetric (in-phase) and antisymmetric (out-of-phase) superposition due to mutual synchronization. At the same time, the external drive causes the phases within the degenerate manifold to be aligned in phase with the drive due to entrainment. In the engine regime, stimulated emission consumes the collective symmetric superposition state, enhancing the population of the *antisymmetric* state. Thus, there is competition between entrainment (in phase) and mutual synchronization (out of phase). In the refrigerator regime, the stimulated absorption enhances the population of the collective *symmetric* superposition state thereby always cooperating with entrainment. Our work sheds light on the synergistic interplay between entrainment and mutual synchronization in quantum systems.

Quantum synchronization in D-level systems.—Quantum synchronization has been studied in systems with continuous degrees of freedom such as oscillators [9–11,13,15,17,39] and discrete degrees of freedom such as spin-1 systems [12,14,20]. A wide variety of measures, based on various physical and mathematical motivations such as phase-space based measures [9,12,20], correlation measures [40], and information-theoretic measures [41] have been used to quantify synchronization.

Here we use the phase-space based measure built on the Husimi-Q representation [42,43] of the steady-state $\rho^{\rm ss}$ with respect to SU(D) coherent state [43,44],

$$Q[\rho^{\rm ss}] = \frac{D!}{\pi^{D-1}}\langle\alpha_D|\rho^{\rm ss}|\alpha_D\rangle, \tag{1}$$

where $|\alpha_D\rangle = \sum_{n=1}^{D}\alpha_n|n\rangle$ is the SU(D) coherent state with coefficients

$$\alpha_n = \begin{cases} e^{i\phi_n}\cos\theta_n\prod_{k=1}^{n-1}\sin\theta_k & 1 \le n < D \\ e^{i\phi_D}\prod_{k=1}^{D-1}\sin\theta_k & n = D. \end{cases} \tag{2}$$

Here it is implicitly assumed that the product term is the identity for $n = 1$ and the reference phase $\phi_D = 0$. The synchronization measure is given by the difference between integrating out the angles θ_k corresponding to the population degrees of freedom and doing the same for the uniform measure, given by

$$\begin{aligned} S(\phi_1,\ldots,\phi_{D-1}) &= \int Q[\rho^{\rm ss}]d\Theta - \frac{1}{(2\pi)^{D-1}} \\ &= \frac{1}{2^{D+1}\pi^{D-2}}\sum_{n\neq m}\rho^{\rm ss}_{nm}e^{i(\phi_m-\phi_n)}, \end{aligned} \tag{3}$$

which lives on a $D-1$ dimensional torus (see the Supplemental Material [45]). The distribution $S(\phi_1,\ldots,\phi_{D-1})$ is zero everywhere for a diagonal steady state which is interpreted as a limit cycle [41] possessing stable amplitudes (fix diagonal elements) but free phases. The notion of free phase in a such diagonal limit cycle is analogous to a classical stochastic limit cycle whose phase distribution approaches a uniform distribution in the steady state [1,13,14,46,47].

We associate the peak of $S(\phi_1,\ldots,\phi_{D-1})$ as a phase-space synchronization measure [12,20,47],

$$S_{\rm max} = \max_{\phi_1,\ldots,\phi_{D-1}}\frac{1}{2^{D+1}\pi^{D-2}}\sum_{n\neq m}\rho^{\rm ss}_{nm}e^{i(\phi_m-\phi_n)}. \tag{4}$$

The synchronization measure, $S_{\rm max}$ only depends on the steady-state coherence. However, we note that a high value of $S_{\rm max}$ requires all phase preferences $\Phi_{ij} = \arg(\rho^{\rm ss}_{ij})$ to be compatible, i.e., $\Phi_{ij} - \Phi_{jk} = \Phi_{ik}\ \forall\ i \neq j \neq k$, in addition to the mere presence of coherence.

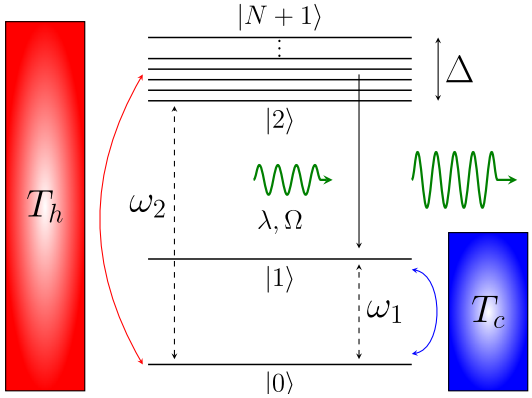

FIG. 1. Schematic of the degenerate quantum thermal maser, which is a generalization of the Scovil–Schulz-DuBois three-level thermal maser. Here, N is the number of states in the degenerate manifold and here we focus on $\Delta = 0$. The near-degenerate case ($\Delta \neq 0$) is discussed in Ref. [50].

Degenerate thermal maser.—Entrainment in quantum systems is the result of an interplay between coherent driving and dissipation [10,12]. The system we consider is depicted in Fig. 1 and consists of $(N+2)$ levels whose bare Hamiltonian is given by

$$H_0 = \omega_1|1\rangle\langle 1| + \sum_{j=2}^{N+1}\omega_j|j\rangle\langle j|, \tag{5}$$

with $\omega_{j+1} \geq \omega_j, (\ \forall\ j = 2,\ldots,N)$ and $\omega_0 = 0$ is the choice of ground-state energy. The upper N levels are degenerate with $\omega_2 = \omega_3 = \cdots = \omega_{N+1}$. Such systems with a large degenerate manifold can be experimentally realized using either rubidium atoms [23] or homonuclear systems often studied in NMR [48,49]. Although we work in the limit of exact degeneracy, our main results hold even in the near-degenerate scenario and will be considered in detail in an accompanying Ref. [50].

This system is driven by a monochromatic drive,

$$V(t) = \sum_{j=2}^{N+1}\lambda_j e^{i\Omega t}|1\rangle\langle j| + \text{H.c.}, \tag{6}$$

with frequency Ω. This drive can be rewritten as a coupling to a collective-transition mode $|1\rangle \leftrightarrow |J\rangle = (1/\lambda_{\rm eff})\sum_j\lambda_j|j\rangle$ with $\lambda_{\rm eff} = \sqrt{\sum_j|\lambda_j|^2}$ being the effective coupling strength. Such collective drives are realizable in an ensemble of atoms driven by light, if the interatomic distance is much smaller than the wavelength of the light, such as in the case of Dicke superradiance [51].

The system is acted upon by a dissipator

$$\mathcal{D}[\rho] = \sum_{\mu=1}^{2}\left[\Gamma_{c_\mu}\mathcal{L}[c_\mu]\rho + \sum_{j=2}^{N+1}\Gamma_{h_\mu}\mathcal{L}[h_\mu^j]\rho\right], \tag{7}$$

which leads to a multilevel generalization of the Scovil–Schulz-DuBois maser heat engine [37,38]. The dissipator $\mathcal{L}[X]\rho = 2X\rho X^\dagger - \{X^\dagger X, \rho\}$ is of the Lindblad form such that the hot (cold) bath with jump operators $h_1^j = h_2^{j\dagger} = |0\rangle\langle j|$ ($c_1 = c_2^\dagger = |0\rangle\langle 1|$) induce transitions between the ground state and the degenerated manifold (first-excited state). The associated rates follow local-detailed balance and are given by $\Gamma_{h_1(c_1)} = \gamma_{h(c)}(1 + n_{h(c)})$ and $\Gamma_{h_2(c_2)} = \gamma_{h(c)} n_{h(c)}$ with $\gamma_{h(c)}$ being the effective system-bath coupling strength and $n_{h(c)} = [\exp(\beta_{h(c)}\omega_{2(1)}) - 1]^{-1}$ being the Bose-Einstein distribution at inverse temperature $\beta_{h(c)}$. The action of the heat baths leads to a population inverted steady state between the first-excited state $|1\rangle$ and the degenerated manifold $|j\rangle$, $\forall\ j = 2, \ldots, N+1$ if $n_h > n_c$. If there is population inversion, the system behaves as a maser heat engine [52]. However, if $n_h < n_c$, population inversion is lost, and the system behaves as a refrigerator by attenuating the drive [52]. We can rewrite the Hamiltonian in a frame corotating with the drive as $\tilde{H} = (\Omega/2)(\sum_{j=2}^{N+1}|j\rangle\langle j| - |1\rangle\langle 1|)$ giving us the rotating frame quantum master equation,

$$\frac{d\tilde{\rho}}{dt} = -i[H_0 - \tilde{H} + \tilde{V}, \tilde{\rho}] + \mathcal{D}[\tilde{\rho}], \tag{8}$$

where $\tilde{O} \equiv e^{-i\tilde{H}t} O e^{i\tilde{H}t}$ ($O = \rho,\ V$) is an operator in the rotated frame with $\tilde{V} = \sum_{j=2}^{N+1}\lambda_j|1\rangle\langle j| + \text{H.c.}$

Competition vs cooperation.—Equation (8) can be solved analytically for the case of homogeneous driving strength $\lambda_j = \lambda$ ($\forall\ j = 2, \ldots, N+1$) and resonant driving $\Omega = \omega_2 - \omega_1$. In this case, the steady-state coherences read as

$$\tilde{\rho}_{1j}^{\text{ss}} = i\frac{\lambda(n_c - n_h)\gamma_c\gamma_h(1 + n_h)}{F(N, n_h, n_c, \gamma_c, \gamma_h, \lambda)}, \tag{9}$$

$$\tilde{\rho}_{jl}^{\text{ss}} = \frac{\lambda^2\gamma_c(n_c - n_h)}{F(N, n_h, n_c, \gamma_h, \gamma_c, \lambda)}, \tag{10}$$

where $j, l = 2, \ldots, N+1$, $j \neq l$ and the function $F(N, n_h, n_c, \gamma_c, \gamma_h, \lambda) = AN^2 + BN + C$ with A, B, and C being positive constants that depend on all remaining parameters (see the Supplemental Material [45]).

The *nondegenerate coherence* ($\tilde{\rho}_{1j}$) is directly induced (i.e., $\propto \lambda$) by the drive whereas the *degenerate coherence* ($\tilde{\rho}_{jl}$) is an indirect consequence ($\propto \lambda^2$) of the collective nature of the drive. Their differences are clear as one transforms back to the original frame in which $\rho_{1j} = \tilde{\rho}_{1j}e^{-i\Omega t}$ and $\rho_{jl} = \tilde{\rho}_{jl}$. The phase preferences induced by ρ_{1j} rotate with the driving frequency while that of ρ_{jl} remain stationary in the original frame. This transformation also emphasizes the frequency locking in this system. Even when the drive's frequency is detuned $\Omega \neq \omega_2 - \omega_1$, the nondegenerate coherences still rotate frequency Ω, implying entrainment, as further corroborated by the Arnold tongue [1] structure of $S_{\max}$ (see the Supplemental Material [45]).

Both these coherences affect the phase distributions of the states within the degenerate manifold. For these reasons, we infer that there are two synchronization mechanisms at play in this system, entrainment induced directly by the drive and mutual coupling that occurs due to the presence of a degenerate manifold. Entrainment induces phases relative to driving whose effect is the emergence of stable nondegenerate coherence $\tilde{\rho}_{1j}^{\text{ss}}$. On the other hand, mutual coupling induces a relative phase between states in the degenerated manifold independent of the driving phase, which is reflected by stable degenerate coherence $\tilde{\rho}_{jl}^{\text{ss}}$.

Recall that we have denoted $\Phi_{ij} = \arg(\tilde{\rho}_{ij}^{\text{ss}})$ as the steady-state phase preferences. When there are multiple such preferences, synchronization requires all the phase relations to be compatible, i.e., $\Phi_{ij} - \Phi_{jl} = \Phi_{il}$ ($i \neq j \neq l$). However, we find that such a condition is only satisfied in the refrigerator regime where $\Phi_{j1} = 3\pi/2$ and $\Phi_{jl} = 0$ for $j, l = 2, 3, \ldots, N+1$ and $j \neq l$. In the engine regime, we have $\Phi_{j1} = \pi/2$ and $\Phi_{jl} = \pi$. We interpret this as a result of an interplay between entrainment and mutual coupling. We find that entrainment always pulls the degenerate states to be *in phase* [Fig. 2(a)]. Meanwhile, mutual coupling prefers out-of-phase configuration in the engine regime [Fig. 2(b)], and in-phase configuration in the refrigerator regime. Consequently, we expect entrainment and mutual coupling to cooperate in the refrigerator regime and compete in the engine regime.

The competition and cooperation are obvious when we calculate the phase space synchronization measure $S_{\max}$ [see Eq. (4)]. In general, this requires optimization over N variables which we calculate analytically for $N = 2$ (see the Supplemental Material [45]):

$$S_{\max} = \frac{1}{16\pi^2} \times \begin{cases} |\tilde{\rho}_{12}^{\text{ss}}| + |\tilde{\rho}_{13}^{\text{ss}}| + |\tilde{\rho}_{23}^{\text{ss}}| & \text{if } n_h < n_c \\ |\tilde{\rho}_{12}^{\text{ss}}| + |\tilde{\rho}_{13}^{\text{ss}}| - |\tilde{\rho}_{23}^{\text{ss}}| & \text{if } n_h > n_c \,\&\, k > 2 \\ \left(1 + \frac{k^2}{2}\right)|\tilde{\rho}_{23}^{\text{ss}}| & \text{if } n_h > n_c \,\&\, k \leq 2, \end{cases} \tag{11}$$

where $k = \gamma_h(1 + n_h)/\lambda = |\tilde{\rho}_{12}^{\text{ss}}|/|\tilde{\rho}_{23}^{\text{ss}}| = |\tilde{\rho}_{13}^{\text{ss}}|/|\tilde{\rho}_{23}^{\text{ss}}|$ is the *dissipation-to-driving* ratio. The set of optimal phases $(\varphi_{21}^{\text{opt}}, \varphi_{31}^{\text{opt}}) \equiv (\varphi_{21}, \varphi_{31})|_{S=S_{\max}}$ evaluated in Ref. [45] are given by

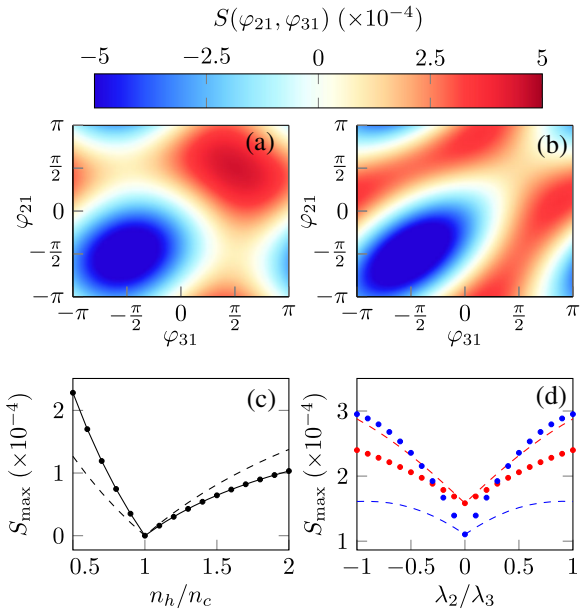

FIG. 2. Interplay between entrainment and mutual coupling for $N = 2$. Panels (a) and (b) show phase quasidistribution function $S(\varphi_{21},\varphi_{31})$ [Eq. (3)] where $\varphi_{ij} = \phi_i - \phi_j$ in the engine regime ($n_h/n_c = 100$). For $k = 3$, $S(\varphi_{21},\varphi_{31})$ shows a localized maximum when the phases are in phase [$\varphi_{21} - \varphi_{31} \approx 0$ in the red region in (a), entrainment dominant]. Whereas for $k = 0.75$, when $S(\varphi_{21},\varphi_{31})$ is maximized the phases do not localize but their difference is out of phase [$\varphi_{21} - \varphi_{31} \approx \pi$ in the red region in (b), mutual coupling dominant]. Panel (c) shows $S_{\max}$ (solid circle) as a function of n_h/n_c with the solid line representing the analytic prediction of Eq. (11). The dashed line is the entrainment contribution to $S_{\max}$, i.e., $(|\rho_{12}| + |\rho_{13}|)/16\pi^2$. The boundary between refrigerator ($n_h/n_c < 1$) and engine ($n_h/n_c > 1$) regime is given by $n_h/n_c = 1$. Panel (d) shows $S_{\max}$ (solid circle) and $(|\rho_{12}| + |\rho_{13}|)/16\pi^2$ (dashed line) plotted against inhomogeneous driving strength ratio $|\lambda_2/\lambda_3| \leq 1$ in the engine (red) and refrigerator (blue) regimes indicating competition (cooperation) between entrainment and mutual coupling is robust in the engine (refrigerator) regime. The other parameter values are $\omega_2 = \omega_3 = 3\omega_1$, $\Omega = \omega_2 - \omega_1$, $\gamma_c = 0.2\omega_1$, $\gamma_h = 0.05\omega_1$, $n_c = 0.5$, and $\lambda_2 = 0.1\omega_1$.

$$(\varphi_{21}^{\text{opt}},\varphi_{31}^{\text{opt}}) = \begin{cases} \left(\frac{3\pi}{2},\frac{3\pi}{2}\right) & \text{if } n_h < n_c \\ \left(\frac{\pi}{2},\frac{\pi}{2}\right) & \text{if } n_h > n_c \,\&\, k > 2 \\ (\chi,\pi-\chi)\,\&\,(\pi-\chi,\chi) & \text{if } n_h > n_c \,\&\, k \leq 2, \end{cases} \tag{12}$$

where $\varphi_{ij} = \phi_i - \phi_j$ and $\chi = \arcsin(k/2)$. Equations (11) and (12) show the effect of the coherent drive and bath couplings on the synchronous dynamics of the system. Cooperation in the refrigerator regime ($n_c > n_h$) is reflected by the fact that each component of the magnitude of coherence adds up in the synchronization measure $S_{\max}$, whereas in the engine case, there is competition since the mutual coupling component $|\tilde{\rho}_{23}^{\text{ss}}|$ reduces the effect of the entrainment contribution $|\tilde{\rho}_{12}^{\text{ss}}| + |\tilde{\rho}_{13}^{\text{ss}}|$. Note that this is different from the previously reported phenomenon of synchronization blockade [14,53]; in our case, $S_{\max}$ cannot vanish except for $\lambda = 0$ or $n_h = n_c$ where the steady state is diagonal (see the Supplemental Material [45]).

In the engine regime, $S_{\max}$ is also divided into regimes where entrainment is dominant ($k > 2$) and where the mutual coupling is dominant ($k < 2$). The phases are either equal in some cases or arranged antipodally in other cases. The transition from entrainment to a mutual coupling dominant regime is shown in Figs. 2(a) and 2(b) where we plot the phase distribution $S(\varphi_{21},\varphi_{31})$ for different k values. In particular, we see that as we cross $k = 2$, the relative phases go from in phase to out of phase. Moreover, the localization pattern changes from a point localization to ring localization (on a torus), wherein the latter only the relative phase $\varphi_{23} = \varphi_{21} - \varphi_{31}$ is fixed, indicating that entrainment is lost.

The competition and cooperation observed is also robust with respect to all values of individual driving strength ratio λ_2/λ_3 as shown in Fig. 2(d). Interestingly, $S_{\max}$ is symmetric with respect to a transformation $\lambda_j \to -\lambda_j$ which transforms $\tilde{\rho}_{jl}^{\text{ss}} \to -\tilde{\rho}_{jl}^{\text{ss}}$ for all $k \neq j$. This can be intuitively explained by $S_{\max}$ only depending on the norm of coherence. In this case, the phase preference of entrainment and mutual coupling is reversed, i.e., both prefer *out of phase* in the refrigerator regime while mutual coupling (entrainment) prefers *in phase* (*out of phase*) in the engine regime.

Scaling with N.—Calculating $S_{\max}$ boils down to performing N-variable optimization which is analytically difficult for $N > 2$. However, in the refrigerator regime, assuming homogeneous driving $\lambda_j = \lambda$ the problem simplifies, and one can show that $S_{\max}$ saturates the l_1-norm bound [41] $S_{\max} \propto C_{l_1} = \sum_{i<j}^{N+1} |\tilde{\rho}_{ij}|$ with optimum phases $\varphi_{j1}^{\text{opt}} = 3\pi/2 \;\; \forall \;\; j \geq 2$ (see the Supplemental Material [45]). The proportionality of $S_{\max}$ with l_1 norm is due to cooperation between entrainment and mutual coupling. Entrainment tends to pull all the phases to $3\pi/2$, and phase-attractive mutual coupling amplifies the effect. Cooperation can also be seen from Fig. 3(b) where we observe scaled synchronization measure $\mathbb{S}_{\max} \equiv (2\pi)^N S_{\max}$ always exceeds the contribution from entrainment for any N. Furthermore, all optimum phases coalesce to a single point $3\pi/2$ [Fig. 3(d)] as predicted analytically. Overall for large N, we predict mutual coupling to dominate $S_{\max}$ since the number of degenerate coherences $\tilde{\rho}_{jl}^{\text{ss}}$ scale as N^2 whereas the nondegenerate coherences scale linearly with N. In the limit $N \to \infty$, we predict that in the refrigerator regime, $\mathbb{S}_{\max}$ approaches a constant that depends only on the baths' properties (see the Supplemental Material [45]),

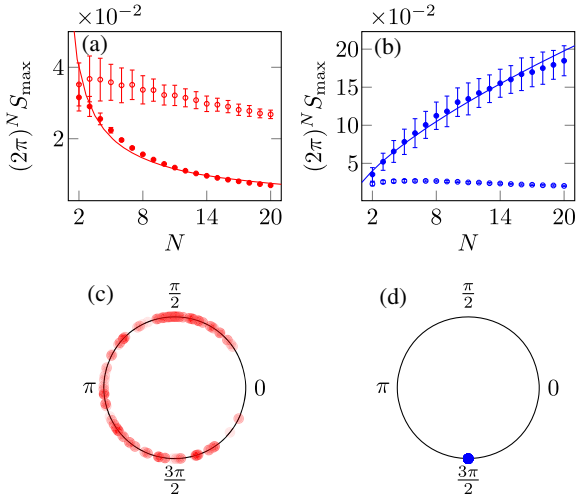

FIG. 3. Panels (a), (b) show $\mathbb{S}_{\max} = (2\pi)^N S_{\max}$ (solid circle) compared with its entrainment contribution $\frac{1}{4}\sum_{j=2}^{N+1} |\rho_{1j}|$ (empty circle) as a function of N. The error bar is calculated from 10^2 random realizations of driving strength ratio $\lambda_j/\lambda_2 \leq 1$ for $\lambda_j \geq 0$ and $j = 3, \ldots, N+1$ with λ_2 held constant. The solid lines are the curve fits using $\mathbb{S}_{\max} \propto N^{\alpha}$ with $\alpha = -0.72$ (a) and $= 0.69$ (b). Panels (c), (d) show optimum phases $\{\varphi_{j1}^{\text{opt}}\}$ for $N = 20$ in the engine [(c), $n_h/n_c = 10$] and refrigerator [(d), $n_h/n_c = 0.4$] regimes plotted on a unit circle. The different opacity represents different realizations of λ_j/λ_2 ($j = 3, \ldots, N+1$). All the phases in all realizations coalesce to a single data point $\varphi_{j1} = 3\pi/2 \ \forall \ j \geq 2$ in the refrigerator case. All other parameters are the same as Fig. 2.

$$\mathbb{S}_{\max} = \lim_{N\to\infty} (2\pi)^N S_{\max}$$
$$n_c \overset{=}{>} n_h \frac{\gamma_c(n_c - n_h)}{8n_h[\gamma_c(1+n_c) + \gamma_h(1+n_h)]}. \tag{13}$$

In the engine case, it is difficult to find an analytic closed-form expression for $\mathbb{S}_{\max}$. However, we observe in Fig. 3(a), that the competition between entrainment and mutual coupling persists for any N. In this regime, the dominant phase repulsive mutual coupling pushes the phases toward uniform distribution as shown in Fig. 3(c). Using this phase uniformity, we analytically (see the Supplemental Material [45]) show that $\mathbb{S}_{\max}$ is zero asymptotically ($N \to \infty$) explaining the decay seen in Fig. 3(a). Thus, in the limit of macroscopic degeneracy, the qualitative behavior of this engine model is analogous to the Kuramoto model with phase-repulsive coupling, where the mean-field synchronization order parameter approaches zero [54].

Summary.—We have shown that there exists an interplay between entrainment and mutual coupling in a collectively driven-dissipative degenerate thermal maser. The interplay depends on the thermodynamic functionality of the maser, i.e., they compete in the engine regime and cooperate in the refrigerator regime. The results rely on two key ingredients: (i) a coherent drive that collectively couples to the degenerate manifold causing entrainment and mutual coupling to coexist and (ii) a dissipative mechanism that causes a population inversion between the nondegenerated and degenerated manifolds to observe the competition.

We demonstrate our findings using a minimal model of a generalized Scovil–Schulz-DuBois maser heat engine and show that in the thermodynamic limit ($N \to \infty$) the dominance of mutual coupling leads to phase repulsiveness causing the engine's working substance to be asynchronized ($\mathbb{S}_{\max} = 0$). On the other hand, since there is cooperation in the refrigerator case, the phases coalesce to $3\pi/2$ giving a finite $\mathbb{S}_{\max}$ that is independent of system properties. In other words, as the system size increases in order for the working substance to be synchronized the external drive needs to perform work on the system.

Our work not only contributes to the growing field of quantum synchronization by adding valuable insights when distinct synchronizing mechanisms coexist but helps one to understand quantum heat engines from a synchronization perspective.

This research was supported by the Institute for Basic Science in South Korea (IBS-R024-Y2). S. V. acknowledges support from a Government of India DST-QUEST Grant No. DST/ICPS/QuST/Theme-4/2019. The authors would like to thank V. Singh for useful discussions.

*sai@phy.iitb.ac.in
†juzar_thingna@uml.edu

[1] A. Pikovsky, M. Rosenblum, and J. Kurths, *Synchronization, a Universal Concept in Nonlinear Sciences* (Cambridge University Press, Cambridge, 2003).
[2] R. Adler, Proc. IRE **34**, 351 (1946).
[3] J. A. Acebrón, L. L. Bonilla, C. J. Pérez Vicente, F. Ritort, and R. Spigler, Rev. Mod. Phys. **77**, 137 (2005).
[4] H. Sakaguchi, Prog. Theor. Phys. **79**, 39 (1988).
[5] L. M. Childs and S. H. Strogatz, Chaos **18**, 043128 (2008).
[6] J. Snyder, A. Zlotnik, and A. Hagberg, Chaos **27**, 103108 (2017).
[7] D. S. Goldobin, A. V. Pimenova, M. Rosenblum, and A. Pikovsky, Eur. Phys. J. Spec. Top. **226**, 1921 (2017).
[8] I. Z. Kiss, Y. Zhai, and J. L. Hudson, Phys. Rev. E **77**, 046204 (2008).
[9] S. Walter, A. Nunnenkamp, and C. Bruder, Phys. Rev. Lett. **112**, 094102 (2014).
[10] T. E. Lee and H. R. Sadeghpour, Phys. Rev. Lett. **111**, 234101 (2013).
[11] A. Chia, L. C. Kwek, and C. Noh, Phys. Rev. E **102**, 042213 (2020).
[12] A. Roulet and C. Bruder, Phys. Rev. Lett. **121**, 053601 (2018).
[13] L. Ben Arosh, M. C. Cross, and R. Lifshitz, Phys. Rev. Res. **3**, 013130 (2021).
[14] M. Koppenhöfer and A. Roulet, Phys. Rev. A **99**, 043804 (2019).

[15] T. E. Lee, C.-K. Chan, and S. Wang, Phys. Rev. E **89**, 022913 (2014).
[16] M. Xu, D. A. Tieri, E. C. Fine, J. K. Thompson, and M. J. Holland, Phys. Rev. Lett. **113**, 154101 (2014).
[17] S. Walter, A. Nunnenkamp, and C. Bruder, Ann. Phys. (Amsterdam) **527**, 131 (2015).
[18] B. Zhu, J. Schachenmayer, M. Xu, F. Herrera, J. G. Restrepo, M. J. Holland, and A. M. Rey, New J. Phys. **17**, 083063 (2015).
[19] J. M. Weiner, K. C. Cox, J. G. Bohnet, and J. K. Thompson, Phys. Rev. A **95**, 033808 (2017).
[20] A. Roulet and C. Bruder, Phys. Rev. Lett. **121**, 063601 (2018).
[21] F. Schmolke and E. Lutz, Phys. Rev. Lett. **129**, 250601 (2022).
[22] M. Koppenhöfer, C. Bruder, and A. Roulet, Phys. Rev. Res. **2**, 023026 (2020).
[23] A. W. Laskar, P. Adhikary, S. Mondal, P. Katiyar, S. Vinjanampathy, and S. Ghosh, Phys. Rev. Lett. **125**, 013601 (2020).
[24] V. R. Krithika, P. Solanki, S. Vinjanampathy, and T. S. Mahesh, Phys. Rev. A **105**, 062206 (2022).
[25] M. Hajdušek, P. Solanki, R. Fazio, and S. Vinjanampathy, Phys. Rev. Lett. **128**, 080603 (2022).
[26] H. Zhou, J. Thingna, P. Hänggi, J.-S. Wang, and B. Li, Sci. Rep. **5**, 14870 (2015).
[27] T. Herpich, J. Thingna, and M. Esposito, Phys. Rev. X **8**, 031056 (2018).
[28] J. Thingna, M. Esposito, and F. Barra, Phys. Rev. E **99**, 042142 (2019).
[29] N. Jaseem, M. Hajdušek, V. Vedral, R. Fazio, L.-C. Kwek, and S. Vinjanampathy, Phys. Rev. E **101**, 020201(R) (2020).
[30] J.-W. Ryu, A. Lazarescu, R. Marathe, and J. Thingna, New J. Phys. **23**, 105005 (2021).
[31] J. Son, P. Talkner, and J. Thingna, PRX Quantum **2**, 040328 (2021).
[32] P. Solanki, N. Jaseem, M. Hajdušek, and S. Vinjanampathy, Phys. Rev. A **105**, L020401 (2022).
[33] J. Son, P. Talkner, and J. Thingna, Phys. Rev. A **106**, 052202 (2022).
[34] C.-M. Kim, S. Rim, W.-H. Kye, J.-W. Ryu, and Y.-J. Park, Phys. Lett. A **320**, 39 (2003).
[35] Y. Kuramoto and D. Battogtokh, Nonlinear Phenom. Complex Syst. **5**, 380 (2002).
[36] D. M. Abrams and S. H. Strogatz, Phys. Rev. Lett. **93**, 174102 (2004).
[37] H. E. D. Scovil and E. O. Schulz-DuBois, Phys. Rev. Lett. **2**, 262 (1959).
[38] K. E. Dorfman, D. Xu, and J. Cao, Phys. Rev. E **97**, 042120 (2018).
[39] A. Mari, A. Farace, N. Didier, V. Giovannetti, and R. Fazio, Phys. Rev. Lett. **111**, 103605 (2013).
[40] F. Galve, G. Luca Giorgi, and R. Zambrini, Quantum correlations and synchronization measures, in *Lectures on General Quantum Correlations and their Applications*, edited by F. F. Fanchini, D. d. O. Soares Pinto, and G. Adesso (Springer International Publishing, Cham, 2017), pp. 393–420.
[41] N. Jaseem, M. Hajdušek, P. Solanki, L.-C. Kwek, R. Fazio, and S. Vinjanampathy, Phys. Rev. Res. **2**, 043287 (2020).
[42] W. P. Schleich, *Quantum Optics in Phase Space* (John Wiley & Sons, New York, 2011).
[43] T. Tilma and K. Nemoto, J. Phys. A Math. Theor. **45**, 015302 (2011).
[44] K. Nemoto, J. Phys. A Math. Gen. **33**, 3493 (2000).
[45] See Supplemental Material at http://link.aps.org/supplemental/10.1103/PhysRevLett.131.030401 for (a) aynchronization in D-level system, (b) steady state of a generalized Scovil–Schulz-DuBois maser, (c) $S_{\max}$ calculation for a generalized Scovil–Schulz-DuBois maser, and (d) proof that $S_{\max} = 0$ if and only if ρ is diagonal ($D = 3$).
[46] C. Kurrer and K. Schulten, Physica (Amsterdam) **50D**, 311 (1991).
[47] H. Eneriz, D. Rossatto, F. A. Cárdenas-López, E. Solano, and M. Sanz, Sci. Rep. **9**, 19933 (2019).
[48] T. S. Mahesh and D. Suter, Phys. Rev. A **74**, 062312 (2006).
[49] S. S. Roy and T. S. Mahesh, Phys. Rev. A **82**, 052302 (2010).
[50] T. Murtadho, J. Thingna, and S. Vinjanampathy, companion paper, Phys. Rev. A **108**, 012205 (2023).
[51] M. Gross and S. Haroche, Phys. Rep. **93**, 301 (1982).
[52] E. Boukobza and D. J. Tannor, Phys. Rev. Lett. **98**, 240601 (2007).
[53] P. Solanki, F. M. Mehdi, M. Hajdušek, and S. Vinjanampathy, arXiv:2212.09388.
[54] L. S. Tsimring, N. F. Rulkov, M. L. Larsen, and M. Gabbay, Phys. Rev. Lett. **95**, 014101 (2005).